Microbes and Infection 26 (2024) 105342

Contents lists available at ScienceDirect

Microbes and Infection

journal homepage: www.elsevier.com/locate/micinf

Original article

Engineering *Mycoplasma pneumoniae* to bypass the association with Guillain-Barré syndrome

Alicia Broto [a, 2], Carlos Piñero-Lambea [a, b, i, 2], Carolina Segura-Morales [a], Anne P. Tio-Gillen [c, d], Wendy W.J. Unger [e], Raul Burgos [a], Rocco Mazzolini [a, b], Samuel Miravet-Verde [a], Bart C. Jacobs [c, d], Josefina Casas [f], Ruth Huizinga [c], Maria Lluch-Senar [a, b, i], Luis Serrano [a, g, h, 1, *]

[a] *Centre for Genomic Regulation (CRG), The Barcelona Institute of Science and Technology, Barcelona, Spain*
[b] *Pulmobiotics Ltd, Dr. Aiguader 88, Barcelona 08003, Spain*
[c] *Department of Immunology, Erasmus MC University Medical Centre, Rotterdam, the Netherlands*
[d] *Department of Neurology, Erasmus MC University Medical Centre, Rotterdam, the Netherlands*
[e] *Department of Pediatrics, Laboratory of Pediatrics, Erasmus MC—Sophia Children's Hospital, University Medical Centre, Rotterdam, the Netherlands*
[f] *IQAC, CSIC, Spain*
[g] *Universitat Pompeu Fabra (UPF), Barcelona, 08002, Spain*
[h] *ICREA, Pg. Lluís Companys 23, Barcelona, 08010, Spain*
[i] *Institute of Biotechnology and Biomedicine "Vicent Villar Palasi" (IBB), Universitat Autònoma de Barcelona, Barcelona, Spain*

ARTICLE INFO

Article history:
Received 6 May 2023
Accepted 19 April 2024
Available online 26 April 2024

Keywords:
Mycoplasma pneumoniae
Glycolipids
Galactocerebrosides
Glycosyltransferases
Immune response
Molecular mimicry

ABSTRACT

A non-pathogenic *Mycoplasma pneumoniae*-based chassis is leading the development of live biotherapeutic products (LBPs) for respiratory diseases. However, reports connecting Guillain-Barré syndrome (GBS) cases to prior *M. pneumoniae* infections represent a concern for exploiting such a chassis. Galactolipids, especially galactocerebroside (GalCer), are considered the most likely *M. pneumoniae* antigens triggering autoimmune responses associated with GBS development. In this work, we generated different strains lacking genes involved in galactolipids biosynthesis. Glycolipid profiling of the strains demonstrated that some mutants show a complete lack of galactolipids. Cross-reactivity assays with sera from GBS patients with prior *M. pneumoniae* infection showed that certain engineered strains exhibit reduced antibody recognition. However, correlation analyses of these results with the glycolipid profile of the engineered strains suggest that other factors different from GalCer contribute to sera recognition, including total ceramide levels, dihexosylceramide (DHCer), and diglycosyldiacylglycerol (DGDAG). Finally, we discuss the best candidate strains as potential GBS-free *Mycoplasma* chassis.

1. Introduction

The emergence of programmed microorganisms as delivery vectors, known as live biotherapeutic products (LBPs), offers an interesting alternative to the systemic administration of therapeutic molecules to treat different conditions [1–3]. While most LBPs have been designed to target diseases in the gastrointestinal tract, the first LBP tailored to treat respiratory conditions was only recently reported [4–6]. This LBP based on an engineered version of *Mycoplasma pneumoniae* shows a great biosafety profile in mice lungs [6]. *M. pneumoniae* WT is generally considered to be a mildly infectious agent, although in few cases it can cause pulmonary and extrapulmonary complications affecting kidneys, skin, or the brain that might require hospital care [7]. Moreover, it cannot be overlooked that in humans, prior infections of *M. pneumoniae* have been indirectly linked to the development of Guillain-Barré syndrome (GBS) [8,9], which could hinder any *M. pneumoniae*-based therapy in humans.

GBS is an acute immune-mediated disease affecting the peripheral nervous system [10]. It typically leads to symmetrical weakness of the limbs and acute flaccid paralysis, and about

* Corresponding author. Centre for Genomic Regulation (CRG), The Barcelona Institute of Science and Technology, Barcelona, Spain.
E-mail addresses: h.huizinga@erasmusmc.nl (R. Huizinga), maria.lluch@pulmobio.com (M. Lluch-Senar), luis.serrano@crg.eu (L. Serrano).
[1] Lead Contact.
[2] These two authors contributed equally to the work.

https://doi.org/10.1016/j.micinf.2024.105342

20–25% of patients eventually require mechanical ventilation. With an incidence of approximately 1–2 per 100,000 people yearly and an estimated 3–10% mortality rate [11], it is a sporadic disorder triggered by a prior bacterial or viral infection. The most frequent antecedent pathogen is *Campylobacter jejuni* [12]. *Mycoplasma pneumoniae* is indirectly associated with between 3 and 14% of GBS cases, typically affecting children or young adults [13]. Remarkably, there are no reported cases of GBS implicating other *Mycoplasma* species (*e.g.*, *Mycoplasma genitalium*).

Molecular mimicry between microbial glycolipids and glycosphingolipids (GSLs) from the nerve fibers is a major driving force behind GBS development [14]. GSLs comprise a heterogeneous group of membrane lipids constituted by a carbohydrate polar head linked through an *O*-glycosidic bond to the C1-hydroxyl of a ceramide (*i.e.*, the complex between a sphingosine and a fatty acid) backbone [15]. The carbohydrate moiety in GSLs varies from a single saccharide to oligosaccharide chains of different complexity. For instance, gangliosides are GSLs especially abundant in the neuronal membranes, that contain one or more residues of sialic acid, a class of sugars with a nine-carbon backbone structure. In contrast, cerebrosides, are much simpler GSLs in which the ceramide backbone is linked to a single hexose, commonly galactose (galactocerobroside or galactosylceramide, GalCer) or glucose (glucocerebroside or glucosylceramide, GlcCer) [16]. Of note, GalCer is the predominant GSL in peripheral nerves and is implicated in the structure and function of the myelinated nerve fibers [17]. Both, gangliosides and cerebrosides seem to be linked to GBS. It is proven that carbohydrate mimicry between *C. jejuni* lipo-oligosacharides (LOS) and human gangliosides (*e.g.*, GM1) can induce anti-ganglioside antibodies resulting in GBS development upon *C. jejuni* infection [18]. Anti-ganglioside antibodies also correlate with a few cases of GBS with prior *M. pneumoniae* infection [19], although the *M. pneumoniae* antecedent is more often associated with anti-galactocerebroside (anti-GalCer) antibodies [9,13,20,21]. Nevertheless, it is not rare to find IgM anti-GalCer antibodies after a common *M. pneumoniae* infection not associated with GBS [9,12,13,20,21]. More recent studies found that IgG anti-GalCer antibodies are associated explicitly with GBS cases (with higher titres relating to more severe cases) [13,22–24], indicating an aberrant class switch from anti-GalCer IgM to IgG may be critical for developing GBS.

M. pneumoniae is a cell-wall free bacterium with a plasma membrane rich in phospholipids and glycolipids, forming a glycocalyx [25]. These glycolipids, contain glucose, galactose or a combination of the two as a carbohydrate moiety linked to either diacylglycerol (DAG) or ceramide to form glycoglycerolipids (GGLs) and GSLs, respectively. Chromatographic analysis of *M. pneumoniae* extracts have shown that among all glycolipids, digalactosyldiacylglycerol (GalGalDAG) is the predominant form in the membranes of this bacterium [26]. For the biosynthesis of glycolipids, *M. pneumoniae* encodes three putative glycosyltransferases (MPN028, MPN075 and MPN483) and a UDP-glucose epimerase (GalE, encoded by *mpn257*) that produces UDP-galactose from UDP-glucose [27,28]. The galactolipids (with a terminal β-galactosyl residue in common) derived from the activity of these enzymes could, under certain circumstances, trigger the autoimmune response observed in GBS cases associated with *M. pneumoniae*. Therefore, for the exploitation of any *M. pneumoniae*-based therapy in humans, it is important to ensure that the engineered chassis will be free of galactolipids, especially GalCer, to guarantee the safety of this LBP [29].

In this work we analysed the glycolipid biosynthetic pathway in *M. pneumoniae* by generating a battery of mutant strains lacking different key genes of the route, and/or expressing glycosyltransferases from other species with preference for UDP-glucose. We used liquid chromatography-high resolution mass spectrometry (LC-HRMS) to obtain the glycolipid profile of whole cell extracts from the different engineered strains. The results demonstrated that we successfully engineered *M. pneumoniae* strains free of GalCer or other galactolipids. We also incubated extracts from these strains with sera from GBS patients and showed that some of them are no longer recognised by anti-GalCer antibodies present on the sera. Finally, we propose the best of these engineered strains as potential GBS-free *M. pneumoniae* chassis.

2. Materials and methods

2.1. Bacterial strains, plasmids and oligonucleotides

The strain M129 was used for wild-type *M. pneumoniae* (ATCC 29342, subtype 1); the strain G37 for wild-type *M. genitalium* (ATCC 33530), and the strain 7784 for wild-type *Mycoplasma agalactiae* (kindly provided by Dr. Christine Citti).

The mutant strains described in this work (Supplementary Table 2) are derived from M129 wild-type strain and were generated following the SURE editing system [30]. Briefly, M129-GP35 or M129-GP35-PtetCre strains were transformed by electroporation as previously described [31] with oligonucleotides designed to delete the coding regions of *mpn028*, *mpn257* or *mpn483* genes (Supplementary Table 3) together with plasmids to select those mutations (Supplementary Table 4). Specifically, for knock-out (KO) of genes *mpn257* and *mpn483*, pLoxPuro plasmid was employed as a selector plasmid. To obtain the Δ028 strain, we combined oligo recombineering and cassette exchange using the selector plasmid pRMCEcatVlox. Although less efficient when compared to standard SURE editing, this strategy relies on two incompatible lox sites instead of one, which enables direct gene replacement avoiding the insertion of the entire plasmid sequence. For strains carrying replacements of gene *mpn483* by nucleotide sequences coding for glycosyltransferases in *Bacillus subtilis* (GenBank: QJR46774.1), *M. genitalium* (GenBank: AAC71559.1), or *M. agalactiae* (GenBank: SBO45562.1), the selector plasmids employed were pLoxPuroBS, pLoxPuroGT or pLoxPuroAG, respectively. In addition, two double mutant strains were engineered in which *mpn257* was deleted, and *mpn483* was either deleted or replaced by the MG517 coding gene of *M. genitalium*. To this end, the Δ257 strain was transformed with pGentaVcre, a suicide vector coding for Vcre recombinase, to excise the puromycin resistance gene from the *mpn257* locus. Subsequently, this intermediate strain was transformed with a tetracycline-resistant transposon vector (pMTnTc^{R}) [32], either empty or carrying the MG517 coding sequence of *M. genitalium*. Finally, these two intermediate strains were cotransformed with the oligonucleotide targeting *mpn483* gene and a selector plasmid based on BxB1 recombinase termed pAttBPuroBxB1.

The location of the MTn carrying the GP35 or GP35-PtetCre cassettes from the parental strains was determined in each strain by A-PCR as previously described [33,34]. Briefly, genomic DNA from the clonal strain with an MTn unknown insertion is used in a low stringency PCR with the primers S6b, with homology to a short fragment inside the MTn, and primer C289 (or C289b) which is a primer with a 5′unic sequence and the 3′ randomised sequence NNNNNNAAAGC(G) ending in a highly repeated sequence in the *M. pneumoniae* genome. Then, PCR products generated were purified as a pool and used as the template in a second PCR to isolate a single fragment with primers S6 and C290. This final fragment is sequenced to determine the insertion site of the MTn. Similarly, the location of the second MTn in the double mutant strains was determined by A-PCR but, in these cases, primer S3 was used instead of S6b or S6.

All plasmids generated in this study (Supplementary Table 4) were assembled following the Gibson method [35] in an *Escherichia coli* host (chemically competent cells #C2987H NEB), and the oligonucleotides employed to this end can be found in Supplementary Table 3.

2.2. Mycoplasma sample preparation and total protein quantification

Mycoplasma strains were cultured in tissue culture flasks (75 cm^2) at 37 °C and 5% CO_2 in the appropriate medium until confluent, but before it was acidified. *M. pneumoniae* strains were cultured in Hayflick medium (pH 7.8); *M. genitalium* (strain G37) in SP4 medium; and *M. agalactiae* (strain 7784) in Hayflick medium supplemented with 0.5% pyruvate with shaking. Cells were washed twice with PBS, harvested and pelleted in a high-speed centrifuge (10,000 g for 10 min). The pellet of cells is then processed differently depending on the needs for the downstream tests, as explained in the following protocols.

For total protein quantification, the pellet of cells was lysed in 100 μl of lysis buffer (4% SDS, 100 mM Hepes) and boiled 10 min at 95 °C. Total protein in the extracts was determined by BCA assay (Pierce, #23225).

2.3. Time-course experiments

M. pneumoniae growth was monitored using a Tecan spark 10M plate reader by determining the growth index (ratio between the absorbance at 430 nm and 560 nm) [27]. *M. pneumoniae* strains (WT, Δ028, Δ483, Δ257, Δ483::GT, Δ483::AG, Δ483::SB, Δ257Δ483::prGT and Δ257Δ483) were inoculated in triplicate in 96-well plates. Total protein in the mycoplasma stocks was determined by BCA assay (Pierce) in order to inoculate the equivalent of 2 μg of total protein in 200 μl medium per sample. Media acidification was measured in a microplate reader. The experiments were performed at 37 °C collecting absorbance reads at 460 nm and 560 nm every 2 h for at least 10 days.

The Lysostaphin activity on the supernatants of the resulting strains was evaluated as previously described [4] with slight modifications. Briefly, Mycoplasma strains were grown in 25-cm2 flasks filled with 4 ml of Hayflick medium. After three days the culture supernatant, with the secreted Lysostaphin, was collected and passed through a 0.22 μm filter. Then, the antimicrobial activity of Lysostaphin was tested in *Staphylococcus aureus* cultures. To begin with, an overnight culture of *S. aureus* was prepared in TSB medium. The culture was then diluted 1:30 in fresh TSB, and 180 μl of this starting culture was added to each well of a 96-well plate. The plate was incubated at 37 °C with 1,080 rpm continuous agitation, and the growth of *S. aureus* was monitored by measuring OD 600 nm every 20 min using a TECAN plate reader. After 5 h, recombinant Lysostaphin or different Mycoplasma supernatant samples were added to the wells and the growth of *S. aureus* was tracked for additional 29 h.

2.4. Proteome analysis by protein mass spectroscopy (MS)

The *M. pneumoniae* pellets of the different strains analysed (prepared as explained above) were resuspended in 50 μl of Urea 6 M, NH_4HCO_3 0.2 M. The samples were sonicated for 10 min at high position with on/off pulses of 30 s (Diagenode bioruptor) and then centrifuged at 4 °C for 10 min at 16000 g. Total protein in the extracts was determined by BCA assay (Pierce) and adjusted them all at 1 μg protein/μl.

For MS sample preparation, in solution digestion samples were reduced with dithiothreitol (30 nmols, 1 h, 37 °C) and alkylated in the dark with iodoacetamide (60 nmol, 30 min, 25 °C). The resulting protein extract was first diluted 1/3 with 200 mM NH_4HCO_3 and digested with 1 μg LysC (Wako, cat # 129−02541) overnight at 37 °C and then diluted 1/2 and digested with 1 μg of trypsin (Promega, cat #V5113) for 8 h at 37 °C. After digestion, peptide mix was acidified with formic acid and desalted with a MicroSpin C18 column (The Nest Group, Inc) prior to LC-MS/MS analysis.

For chromatographic and mass spectrometric analysis, samples were analysed using an LTQ-Orbitrap Velos Pro mass spectrometer (Thermo Fisher Scientific, San Jose, CA, USA) coupled to an EASY-nLC 1000 (Thermo Fisher Scientific (Proxeon), Odense, Denmark). Peptides were loaded onto the 2-cm Nano Trap column with an inner diameter of 100 μm packed with C18 particles of 5 μm particle size (Thermo Fisher Scientific) and were separated by reversed-phase chromatography using a 25-cm column with an inner diameter of 75 μm, packed with 1.9 μm C18 particles (Nikkyo Technos Co., Ltd. Japan). Chromatographic gradients started at 93% buffer A and 7% buffer B with a flow rate of 250 nl/min for 5 min and gradually increased 65% buffer A and 35% buffer B in 120 min. After each analysis, the column was washed for 15 min with 10% buffer A and 90% buffer B. Buffer A: 0.1% formic acid in water. Buffer B: 0.1% formic acid in acetonitrile.

The mass spectrometer was operated in positive ionization mode with nanospray voltage set at 2.1 kV and source temperature at 300 °C. Ultramark 1621 was used for external calibration of the FT mass analyser prior the analyses, and an internal calibration was performed using the background polysiloxane ion signal at m/z 445.1200. The acquisition was performed in data-dependent adquisition (DDA) mode and full MS scans with 1 micro scans at resolution of 60,000 were used over a mass range of m/z 350−2000 with detection in the Orbitrap. Auto gain control (AGC) was set to 1E6, dynamic exclusion (60 s) and charge state filtering disqualifying singly charged peptides was activated. In each cycle of DDA analysis, following each survey scan, the top twenty most intense ions with multiple charged ions above a threshold ion count of 5000 were selected for fragmentation. Fragment ion spectra were produced via collision-induced dissociation (CID) at normalised collision energy of 35% and they were acquired in the ion trap mass analyser. AGC was set to 1E4, isolation window of 2.0 m/z, an activation time of 10 ms and a maximum injection time of 100 ms were used. All data were acquired with Xcalibur software v2.2.

Digested bovine serum albumin (New england biolabs cat #P8108S) was analysed between each sample to avoid sample carryover and to assure stability of the instrument and QCloud [36] has been used to control instrument longitudinal performance during the project.

For data analysis, acquired spectra were analysed using the Proteome Discoverer software suite (v2.0, Thermo Fisher Scientific) and the Mascot search engine (v2.6, Matrix Science [37]). The data were searched against a *Mycoplasma pneumoniae* database plus proteins Cat, Par, TcR, MG517, MAGA_RS00300, UgtP, a list of common contaminants (87076 entries) [38] and all the corresponding decoy entries. For peptide identification a precursor ion mass tolerance of 7 ppm was used for MS1 level, trypsin was chosen as enzyme and up to three missed cleavages were allowed. The fragment ion mass tolerance was set to 0.5 Da for MS2 spectra. Oxidation of methionine and N-terminal protein acetylation were used as variable modifications whereas carbamidomethylation on cysteines was set as a fixed modification. False discovery rate (FDR) in peptide identification was set to a maximum of 5%.

Peptide quantification data were retrieved from the “Precursor ion area detector” node from Proteome Discoverer (v2.0) using 2 ppm mass tolerance for the peptide extracted ion current (XIC).

The obtained values were used to calculate protein top 3 area with the unique peptide for protein ungrouped.

The mass spectrometry proteomics data have been deposited to the ProteomeXchange Consortium via the PRIDE [39] partner repository with the dataset identifier PXD039720.

2.5. Dot blot

Mycoplasma samples were prepared as explained above. In this case, the pellets were resuspended in 50 μl SDS 4%, Hepes 100 mM. The samples were sonicated for 10 min at high position with on/off pulses of 30 s (Diagenode bioruptor). Protein levels were quantified using the BCA kit. Samples were treated with 2.5 μg proteinase K/μL of sample (Lucigen #MPRK092) at 65 °C for 15 min, and then at 95 °C for 15 min to inactivate the proteinase K.

One μg of each lysate was loaded into a PVDF membrane previously hydrated with methanol. The membrane was blocked with 5% dry milk in T-TBS (50 mM Tris, 0.5 M NaCl, 0.05% Tween-20, pH 7.4) for 1 h at room temperature and then incubated with primary antibody at 4 °C overnight in T-TBS. Antibodies used were anti-galactocerebroside delipidised whole antiserum (Merck #G9152) at 1:50, and anti-MPN142/p90 (#65114, kindly provided by Prof. R. Herrmann) at 1/1000. The membrane was washed three times with T-TBS during 5 min and incubated with anti-Rabbit IgG (whole molecule)—Peroxidase antibody produced in goat (Sigma #A0545) as the secondary antibody for 1 h at room temperature. After three washes of 5 min with T-TBS the signal was assessed in an iBright.

2.6. Analysis of lipid and glycolipid content in M. pneumoniae cell extracts by liquid chromatography-high resolution mass spectrometry (LC-HRMS)

Mycoplasma whole-cell extracts were prepared from pellets (as explained above) resuspended in 100 μl H_2O and sonicated for 10 min at high position with on/off pulses of 30 s (Diagenode bioruptor). Total protein in the mycoplasma extracts was determined by BCA assay (Pierce). Samples were adjusted to 500 μg protein in 100 μl H_2O and then added 250 μl of methanol to each sample.

Lipids in the mycoplasma extracts were analysed as previously described [40,41] with minor modifications. In detail: **Phospholipids and neutral lipids,** a total of 500 μl of a methanol-chloroform (1:2, vol/vol) solution containing internal standards (16:0 D31_18:1 phosphocholine, 17:0 D5_17:0 diacylglycerol, 17:0/17:0/17:0 triacylglycerol, 0.2 nmol each, from Avanti Polar Lipids) were added to 0.5 mg of mycoplasma lysates. Samples were vortexed and sonicated until they appeared dispersed and extracted at 48 °C overnight. The samples were then evaporated and transferred to 1.5 ml Eppendorf tubes after adding 0.5 ml of methanol. Samples were evaporated to dryness and stored at −80 °C until analysis. Before analysis, 150 μl of methanol were added to the samples, centrifuged at 13,000 g for 3 min, and 130 μl of the supernatants were transferred to ultra-performance liquid chromatography (UPLC) vials for injection and analysis. **Sphingolipids,** a total of 750 μl of a methanol-chloroform (2:1, vol/vol) solution containing internal standards (N-dodecanoylsphingosine, N-dodecanoylglucosylsphingosine, N-dodecanoylsphingosylphosphorylcholine, C17-dihydrosphingosine and C17-dihydrosphingosine-1-phosphate, 0.2 nmol each, from Avanti Polar Lipids) were added to 0.5 mg of mycoplasma lysates. Samples were extracted at 48 °C overnight and cooled. Then, 75 μl of 1 M KOH in methanol was added, and the mixture was incubated for 2 h at 37 °C. After adding 75 μl of 1 M acetic acid, samples were evaporated to dryness and stored at −80 °C until analysis. Before analysis, 150 μl of methanol were added to the samples, centrifuged at 13,000 g for 5 min and 130 μl of the supernatant were transferred to a new vial and injected.

Lipids were analysed by liquid chromatography-high resolution mass spectrometry (LC-HRMS). LC-HRMS analysis was performed using an Acquity ultra-high-performance liquid chromatography (UHPLC) system (Waters, USA) connected to a Time of Flight (LCT Premier XE) Detector. Full scan spectra from 50 to 1800 Da were acquired, and individual spectra were summed to produce data points each of 0.2 s. Mass accuracy at a resolving power of 10,000 and reproducibility were maintained using an independent reference spray via the LockSpray interference. Lipid extracts were injected onto an Acquity UHPLC BEH C8 column (1.7 μm particle size, 100 mm × 2.1 mm, Waters, Ireland) at a flow rate of 0.3 ml/min and a column temperature of 30 °C. The mobile phases were methanol with 2 mM ammonium formate and 0.2% formic acid (A)/water with 2 mM ammonium formate and 0.2% formic acid (B). A linear gradient was programmed as follows: 0.0 min: 20% B; 3 min: 10% B; 6 min: 10% B; 15 min: 1% B; 18 min: 1% B; 20 min: 20% B; 22 min: 20% B. Chromatographic separation of GlcCer and GalCer was achieved using a HILIC column, as described by Boutin et al. [42]. Identification of compounds was based on the accurate mass measurement with an error <5 ppm and its LC retention time, compared with that of a standard (92%). Quantification was carried out using the extracted ion chromatogram of each compound, using 50 mDa windows. The linear dynamic range was determined by injecting internal and natural standards mixtures. Since standards for all identified lipids were not available, the amounts of lipids are given as pmol equivalents relative to each specific standard. Sphingolipids (ceramide; SM, sphingomyelin; and glycoCer: MHCer, monohexosylceramide; and DHCer, dihexosylceramide), glycerophospholipids (PC, phosphatidylcholine), diacylglycerol (DAG), monoglycodiacylglycerol (MGDAG), diglycodiacylglycerol (DGDAG) and triacylglycerol (TAG) were annotated using "C followed by the total fatty acyl chain length:total number of unsaturated bonds" and the "lipid subclass" (*e.g.*, C32:2-PC). The following natural standards were used for the identification of MGDAG (MGlcDAG-C34:1 from *E. coli*, MGDAG-C34:6 from plant and the hydrogenated form MGDAG-C34:0) and DGDAG (DGDAG-C36:6 from plant and the hydrogenated form DGDAGC36:0).

2.7. Serum reactivity with M. pneumoniae glycolipids

Lipids were extracted from wild-type *M. pneumoniae* M129 and glycolipids were visualized using thin-layer chromatography and orcinol staining as described previously [43]. Glycolipids were further fractionated using silica column chromatography and eluted with acetone/hexane/water (220:80:14 v/v/v). Fractions corresponding to mono-, di- and tri-hexose containing glycolipids were subsequently spotted in triplicate onto glass slides covered with polyvinylidene difluoride membranes using a thin-layer chromatography autosampler (CAMAG). Slides were blocked with PBS/2% BSA and incubated with sera (diluted 1:1000), or intravenous immunoglobulins (20 μg/ml) in PBS/1% BSA. Bound IgG antibodies were detected using Cy3-conjugated goat anti-human IgG (Jackson ImmunoResearch). Mean fluorescence intensities were measured using LuxScan™ software.

2.8. Inibition ELISA assay

Mycoplasma samples were prepared as explained above. In this case, the pellets were washed three times with 30 ml sterile PBS (centrifuge 10,000 g for 20 min each time) and then, resuspended in 200 μl of PBS. Total protein in the extracts was determined by BCA assay (Pierce). All samples were adjusted to 4 μg of protein per μL of sample prior to heat-inactivation during 30 min at 56 °C.

Then, all samples were treated with 2.5 μg of proteinase K per μL of sample at 65 °C for 15 min, and then at 95 °C for 15 min to heat inactivate the proteinase K.

Patients with GBS, positive for *M. pneumoniae* and GalCer IgG antibodies were selected from a previous study [22]. Sera were collected before start of treatment with intravenous immunoglobulins (IVIg) and used at 1:200 (anti-GalCer IgG titer 400) or 1:400 (anti-GalCer IgG titer 1600) to reach a ΔOD of 0.5–1 for anti-GalCer IgG. At these dilutions anti-GalCer IgM remained negative (anti-GalCer IgM titers were 100 and 200 respectively). Sera were negative for GM1, GM2, GD1a, GD1b and GQ1b (IgM and IgG). The inhibition ELISA was carried out as described previously [22]. Briefly, half-area 96-well plates were coated with 450 pmol/well GalCer (β-D-galactosylceramide purified from bovine brain; Sigma–Aldrich #C4905) dissolved in 100% ethanol. Control wells contained only ethanol. After evaporation, wells were blocked with PBS pH 7.8 with 1% BSA for 2 h at room temperature and 2 h at 4 °C. Diluted sera were pre-incubated for 3 h at 4 °C on a roller bank with 6.25–25 μg/ml proteinase K-treated *M. pneumoniae* extracts prepared as described above, or with PBS only as reference. Following centrifugation (3000 g, 5 min) supernatants were added to GalCer or ethanol-coated wells. To rule out non-specific antibody depletion, a serum from a patient with GBS (Miller Fisher variant) positive for anti-GQ1b antibodies was preincubated with *Mycoplasma pneumonia* extracts and added to wells coated with 300 pmol GQ1b (Divbio Science #BCR6556-1). Plates were incubated O/N at 4 °C. Wells were washed 6 times with PBS and incubated with HRP-conjugated rabbit anti-human IgG (Jackson Immunoresearch) for 90 min at room temperature. Plates were washed 6 times with PBS, developed with o-phenylenediamine (Sigma) and stopped after 10 min with 2N HCl. Absorbance was measured at 490 nm using a Versamax microplate reader. ΔOD was calculated by subtracting $OD_{Ethanol}$ from OD_{GalCer} or OD_{GQ1b}. Inhibition was calculated as follows:

$$\frac{\Delta OD_{(\text{serum without Mp antigen})} - \Delta OD_{(\text{serum with Mp antigen})}}{\Delta OD_{(\text{serum without Mp antigen})}} x100.$$

3. Results

3.1. Glycolipid metabolic map of M. pneumoniae and its essentiality

To rationally engineer *M. pneumoniae* strains that will not trigger auto-immune responses linked to GBS, we focus our attention on the glycolipid metabolism of this bacterium (Fig. 1). *M. pneumoniae* can synthesise glycolipids using either DAG or ceramide as lipid precursors. The enzymes involved in DAG biosynthesis are essential [44,45]. In contrast, exogenous ceramide or sphingomyelin (SM), a lipid-containing ceramide, can be incorporated directly into the membrane [46]. Despite galactolipids are the main glycolipids found in their membranes, *M. pneumoniae* cells have little to no ability to take up galactose [26]. Therefore, galactose must be synthesised from glucose in a set of four different catalytic reactions (Fig. 1). The first two steps of this pathway are catalysed by essential enzymes as they are responsible for generating Glucose-6-phosphate and Glucose-1-phosphate, the precursors of glycolysis and nucleotide metabolism, respectively [28,44]. Conversely, the two-step conversion of Glucose-1-phosphate to UDP-Galactose is catalysed by GtaB (gene *mpn667*) and GalE (gene *mpn257*) enzymes, whose inactivation produces a fitness phenotype [45]. Finally, for lipid glycosylation, *M. pneumoniae* encodes three putative glycosyltransferases: MPN028, MPN075 and MPN483 [47], of which only suppression of MPN483 results in a fitness phenotype [45]. The other two glycosyltransferases (MPN028 and MPN075), which are very similar to MPN483 (Suppl. Fig. S1A), are expressed at low protein levels (Table 1) and are non-essential under *in vitro* growth conditions [45]. The MPN483 enzyme is a processive and promiscuous glycosyltransferase (CAZy GT2 family member) responsible for synthesising, at least *in vitro,* most of the identified glycolipids in *M. pneumoniae* [47]. It has been shown that, at least *in vitro*, MPN483 uses preferentially DAG but also ceramide as acceptor substrates, and UDP-galactose and less frequently UDP-glucose as donor. Hence, mainly GalDAG but also GalCer and the corresponding dihexoside and trihexoside variants (MGDAG, DGDAG and TGDAG for monohexoside, dihexoside and trihexoside DAG variants, and MHCer, DHCer and THCer for the corresponding ceramide variants) are the main products of MPN483 activity. The MPN075 enzyme showed no activity with either UDP-glucose or UDP-galactose with any acceptor substrates like DAG, ceramide, MGDAG or MHCer, tested *in vitro* [47]. The role of MPN028 is not clear yet, since it could not be expressed at significant levels in *E. coli* [47]. It is possible that the MPN028 plays a role in incorporating the first UDP-hexose in the biosynthesis of glycolipids as the preferred substrates for MPN483 are monoglycosylDAG (MGDAG) glycolipids [47].

3.2. Engineering M. pneumoniae glycolipid biosynthetic pathway to avoid the production of galactolipids

As galactolipids have been suggested as a causative factor of GBS associated with *M. pneumoniae* infection, we designed two strategies to avoid its biosynthesis. The first approach involved the deletion of the *mpn257* gene coding for GalE epimerase to prevent the production of UDP-galactose and, hence, prevent galactolipids synthesis. Since MPN483 strongly prefers UDP-galactose to decorate ceramide or DAG backbones [47], this approach could impair bacterial growth. The second strategy relied on the deletion of *mpn483* gene, coding for the primary glycosyltransferase MPN483, that mainly uses galactose as sugar donor. Nevertheless, as glycosylDAGs (containing either galactose or glucose) are critical components of the membrane [48] and most of them seem to be synthesised by this enzyme [47], this strategy might also impair growth.

To bypass the possible bacterial growth limitations of these two strategies, we also generated strains replacing *mpn483* by an orthologous gene coding for a glycosyltransferase with preferential use of UDP-glucose and, ideally, no use of UDP-galactose. For this, we chose three orthologous gene candidates. The first one is *mg517* from the closely related species *M. genitalium.* The enzyme MG517 sequentially produces MGDAG and DGDAG with a preference for glucosylDAG (GlcDAG) as substrate [49]. For the second candidate, we looked for a related *Mycoplasma* species with *mpn483* orthologues and no orthologues of *mpn257.* In this case, we expect the glycosyltransferase to use preferentially UDP-glucose as the corresponding Mycoplasma species must be unable to make UDP-galactose. One such species is *M. agalactiae* [31,50], with several glycosyltransferases related to MPN483, with the one encoded by the *maga_RS00300* gene showing the highest sequence homology to MPN483 (Suppl. Fig. S1B). Finally, as the third candidate, we chose the UgtP enzyme from *B. subtilis*. This UgtP is a processive glycosyltransferase that transfers glucose from UDP-glucose to DAG [51]. It must be noted that there is no information about using ceramide as a substrate instead of DAG for these three proteins. Additionally, we deleted the *mpn028* gene to test whether it has a

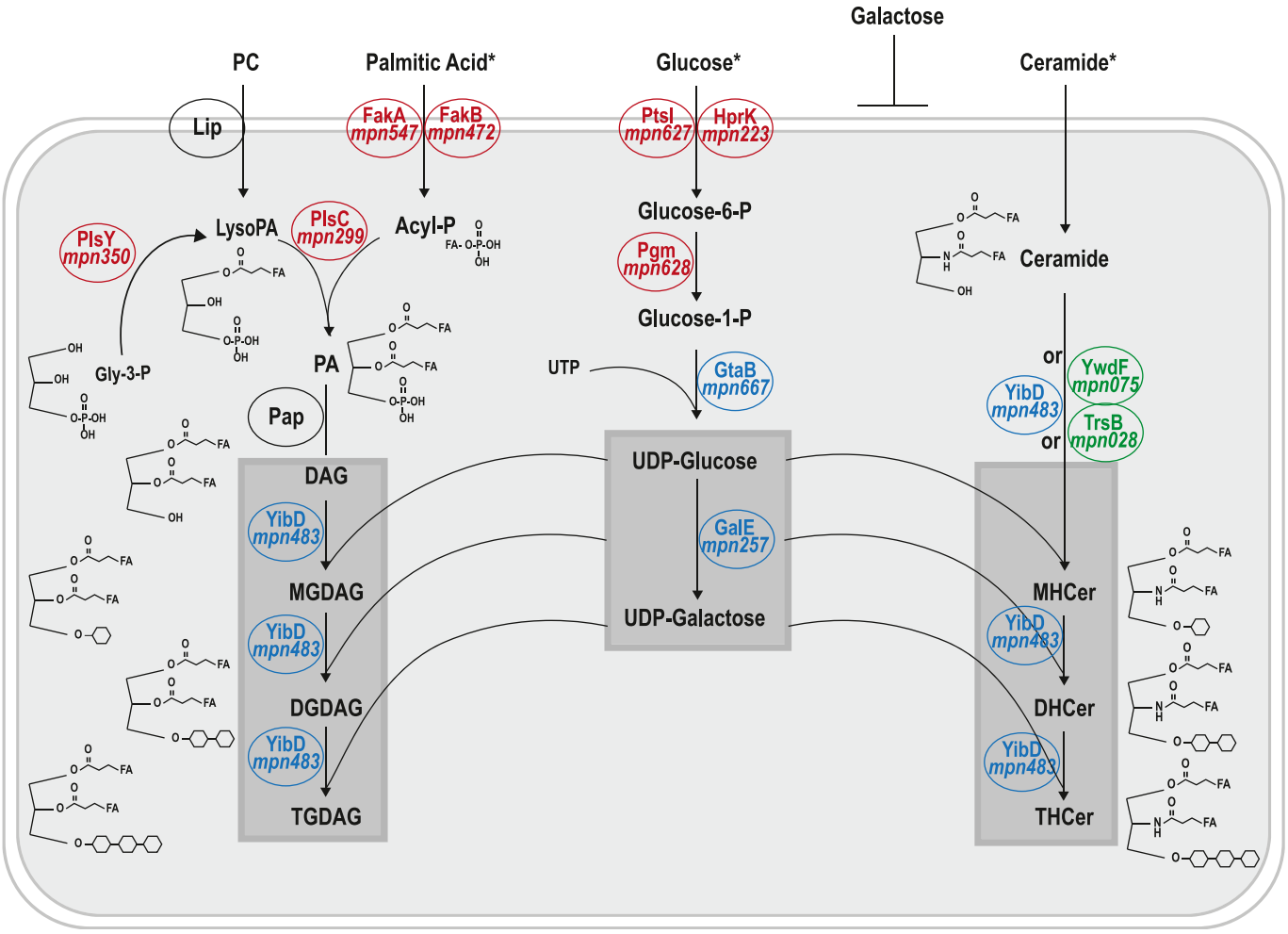

Fig. 1. Glycolipids metabolism of *M. pneumoniae* and its essentiality. Enzymes (inside circles) are coloured according to their essentiality (red for essential, blue for fitness and green for non-essential genes). Gene identifier is also included when the protein activity has been linked to a specific gene in *M. pneumoniae*. Predicted protein activities (Lip: lipase, Pap: phosphatidate phosphatase) lack gene identifier and are coloured in black as their essentiality character is not known. A scheme depicting the structure of the most relevant compounds is shown close to their names. An asterisk (*) highlights compounds demonstrated as precursors for galactolipids by *M. pneumoniae*. Compounds in the map: PC, Phosphatidylcholine; Gly-3-P, Glycerol-3-Phosphate; LysoPA, Lyso Phosphatidic Acid; PA, Phosphatidic Acid; Acyl-P, Acyl-phosphate; Glc-6-P, Glucose-6-Phosphate; Glc-1-P, Glucose-1-Phosphate; DAG, Diacylglycerol. Glycolipids: MGDAG, MonoglycosylDAG (GalDAG or GlcDAG); DGDAG, DiglycosylDAG; TGDAG, TriglycosylDAG; MHCer, Cerebrosides (GalCer or GlcCer); DHCer, Dihexosylceramide; THCer, Trihexosylceramide.

Table 1
Glycosyltransferases and epimerase expression levels in the engineered *M. pneumoniae* strains and the M129 wild-type (WT) strain, as determined by Protein Mass Spectroscopy (MS). Protein quantities (as $\log_2$ values) relate to the area under the curve in the MS spectra for the average of the three best flying peptides in each case, normalised by the median of the set.

	MPN257		MPN028		MPN075		MPN483		Heterologous glycosyltransferase		
	mean	SD	mean	SD	mean	SD	mean	SD	Protein	mean	SD
WT	27,48	0,11	23,55	0,21	24,32	0,02	26,61	0,07	–		
Δ028	27,11		ND		24,57		26,31		–		
Δ257	ND		27,66*	0,16	24,17	0,20	27,25	0,17	–		
Δ483	27,39	0,15	23,19	0,56	24,71	0,31	ND		–		
Δ483::GT	27,68	0,16	25,01	0,46	24,77	0,22	ND		MG517:	30,89	0,44
Δ483::AG	27,63	0,21	24,13	0,19	23,94	0,13	ND		MAGA_RS00300:	29,99	0,23
Δ483::BS	27,65	0,15	24,33	0,52	25,21	0,24	ND		UgtP:	28,27	0,06
Δ257Δ483::prGT	ND		27,49*	0,17	24,18	0,22	ND		MG517:	29,74	0,04
Δ257Δ483	ND		27,59*	0,22	23,85	0,38	ND		–		

Mean values and standard deviation (SD) from a minimum of two bio-replicates (except, only one replicate for the strain Δ028). ND, not detected. An asterisk (*) indicates the difference to WT is statistically significant based on a T-test (P-value<0.05). P-values are listed in the Suppl. Table T1.

role in incorporating the first hexose into the glycolipids. This strategy might limit the glycolipid production in *M. pneumoniae* given that the preferred substrate of MPN483 are glycolipids already containing one sugar residue [47].

Using the new target genome engineering technology for *M. pneumoniae* [30], we successfully generated a set of clonal strains to test all the strategies discussed above. On the one hand, we engineered the strains Δ257, Δ483 and Δ028 with single

deletions of the genes *mpn257*, *mpn483* and *mpn028*, respectively. On the other hand, we engineered three complemented strains named Δ483::GT, Δ483::AG and Δ483::BS in which *mpn483* was replaced by *mg517, maga00300* or *ugtP* genes, respectively. Additionally, we engineered two double mutant strains: the strain Δ257Δ483 missing genes *mpn257* and *mpn483*, and the strain Δ257Δ483::prGT with the same double deletion complemented with the gene *mg517* from *M. genitalium*, under control of the *mpn483* original promoter (see Material and methods for details).

3.3. Growth analysis and proteomic characterisation of strains engineered to impair galactolipid production

Growth curves of the engineered strains showed the expected profile considering their annotation on essentiality studies (Fig. 2). Strains carrying deletions on the fitness genes *mpn483* or *mpn257* showed impaired growth compared to WT, especially in the case of the Δ483 strain. In contrast, growth of strain Δ028 missing the non-essential gene *mpn028* is only slightly slower than that of WT (Fig. 2A). The replacement of *mpn483* with any of the assessed glycosyltransferase coding genes restore growth to almost normal rates (Fig. 2B). The double deletion of *mpn257* and *mpn483* had a similar negative impact on growth as observed for the single deletion of *mpn483*, indicating that there is no significant synergism or additive effects. The introduction of the *mg*517 gene in the double deletion mutant (Δ257Δ483::prGT) improved growth significantly (Fig. 2C).

We also characterised the proteome of the different strains by mass spectroscopy (Table 1, Suppl. Fig. S2 and Suppl. File F2). Most of the strains showed no obvious significant changes on the protein levels except those derived from the corresponding deletions in each strain. However, all strains carrying deletions on the *mpn257* gene showed a significant overexpression of MPN028 (Table 1). This suggests a role of this glycosyltransferase in incorporating UDP-glucose whose levels should be increased in strains lacking the MPN257 glucose epimerase.

Finally, considering that deletions of genes *mpn257* or *mpn483* and the insertion of genes coding for other orthologous glycosyltransferases affect the growth rate and alter the glycolipid profile of the resulting strains (see below), we aimed to assess whether therapeutic molecules were still secreted by the engineered strains at competitive levels. To this end, based on our recent research [4], we transformed a set of strains (*i.e.* WT, Δ257Δ483 and Δ257Δ483::prGT) with a transposon vector coding for the Lysostaphin coding gene fused to a secretion signal and the supernatants of the resulting strains were added to an actively growing *S. aureus* culture. The results show that supernatants collected from all *M. pneumoniae* recombinant strains had an antimicrobial effect against *S. aureus* growth, indicating that these strains were indeed secreting Lysostaphin. However, no effect was observed after adding the supernatant from the *M. pneumoniae* WT strain. This demonstrates that strains carrying the double deletion (Δ257Δ483) or the double deletion complemented with an orthologous glycosyltransferase (Δ257Δ483::prGT) retained their therapeutic effect, at least against *S.aureus* cultures. However, while the antimicrobial activity of the complemented and the WT strain carrying the lysostaphin construct was similar, in the non-complemented strain the effect of supernatant addition takes longer to be observed, possibly due to a lower concentration of antimicrobial in the supernatant due to its impaired growth rate (Supp. Fig. S3).

3.4. Glycolipid profiling of the different strains

We analysed the glycolipid content of the strains to determine the effect of the different gene deletions and replacements on galactolipid production (Fig. 3). We quantified sphingolipids (SM and ceramide); glycerophospholipids (DAG; TAG, triacylglycerol; and PC, phosphatidylcholine); GSLs (MHCer and DHCer); and GGLs (MGDAG and DGDAG) in whole-cell extracts from all strains and WT by liquid chromatography-high resolution mass spectrometry (LC-HRMS). Moreover, we quantified the levels of cerebroside with galactose (GalCer) or glucose (GlcCer) individually, but we could not determine the carbohydrate moieties linked to MGDAG, DGDAG or DHCer due to the technical limitations inherent to the experimental approach. We also looked at the relative abundance of different ceramides and DAGs compounds in the lipids in the different strains, but we did not see any significant differences (Suppl. File F3).

As expected, we found no GalCer in strain Δ257 corroborating that *M. pneumoniae* has no other epimerase able to produce UDP-galactose aside from MPN257 (Fig. 3). This strain shows a slight increase in the amounts of free DAG and Ceramide. However, the more evident changes are related to the increase of monohexoside variants (GlcCer and, especially, MGDAG) and a concomitant decrease in dihexoside variants (DGDAG and DHCer), which can be presumed to be exclusively decorated with glucose, although the specific carbohydrate moieties on MGDAG, DGDAG and DHCer cannot be determined. These results support the reduction of MPN483 activity when only UDP-glucose is available, as observed *in vitro* [47]. Of note, the observed overexpression of MPN028 seen in strain Δ257 by mass spectroscopy might be responsible for the increased GlcCer levels and thus suggests that this glycosyltransferase prefers UDP-glucose as hexose donor.

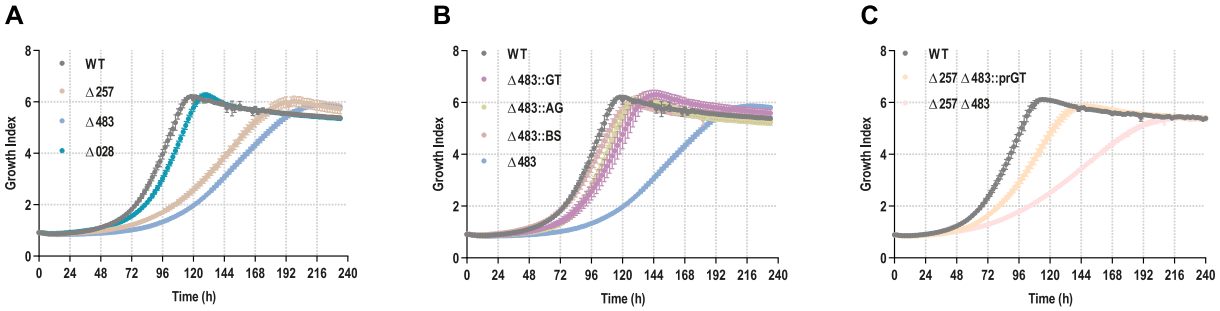

Fig. 2. Growth kinetics of the different strains engineered in this work. Growth was monitored by pH changes in the medium due to lactate and acetate secretion by *M. pneumoniae*. Graphs show growth kinetics (growth index corresponds to the ratio Abs430nm/Abs560nm) of (A) the three knock out strains Δ257, Δ483 and Δ028 compared to the *M. pneumoniae* M129 wild-type strain (WT); (B) the three strains Δ483::GT, Δ483::AG and Δ483::BS with *mpn483* replacement by an orthologous gene compared to the WT and Δ483 strains; (C) the double mutant strains Δ257Δ483 and Δ257Δ483::prGT; compared to the WT strain. Mean values from three bio-replicates. Error bars indicate standard deviation (SD). Source and processed data provided in the suppl. File F1.

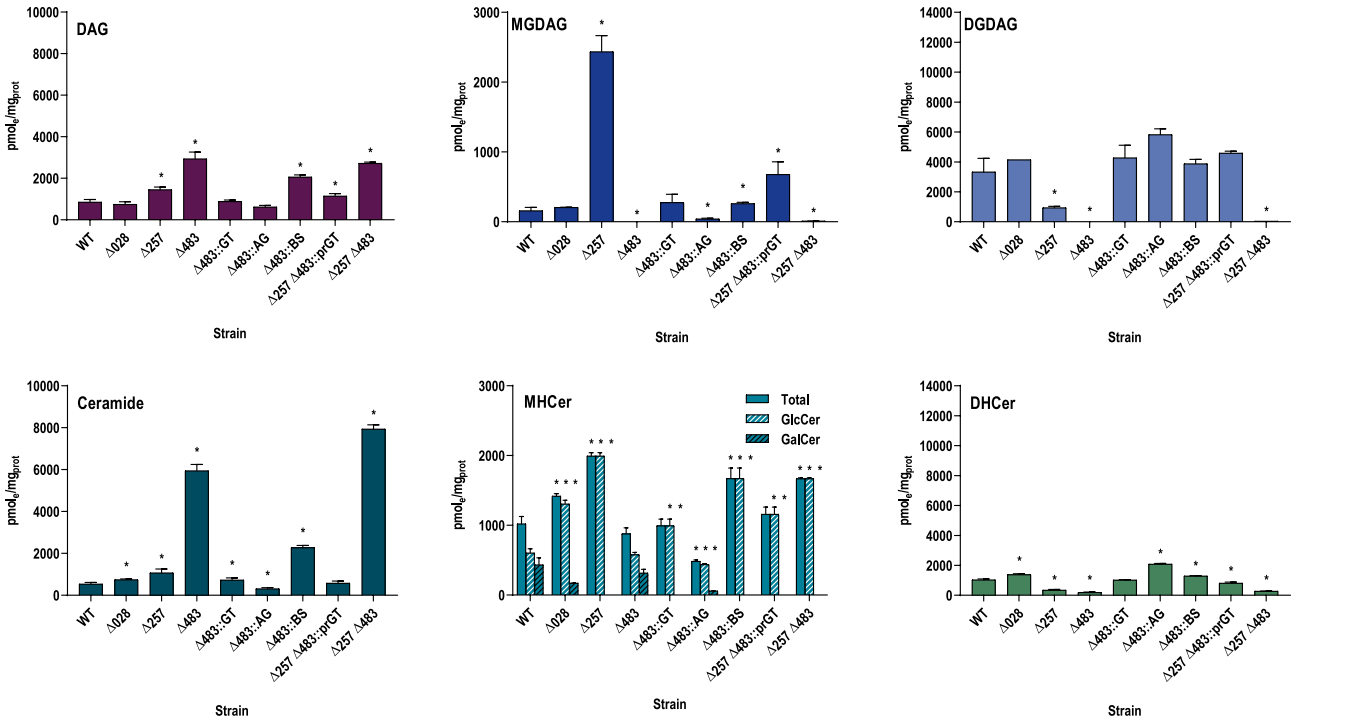

Fig. 3. Glycolipid profiling of the engineered strains by liquid chromatography-high resolution mass spectrometry (LC-HRMS). Quantification of diacylglycerol (DAG), monoglycosylDAG (MGDAG), diglycosylDAG (DGDAG), ceramide, total cerebrosides (MHCer) and dihexosylceramide (DHCer) in mycoplasma extracts from strains Δ028, Δ257, Δ483, Δ483::GT, Δ483::AG, Δ483::SB, Δ257Δ483::prGT, Δ257Δ483 and *M. pneumoniae* M129 wild-type strain (WT). Galactocerebroside (GalCer) and glucocerebroside (GlcCer) were also quantified individually. Graphs show lipid concentration in pmol equivalent per mg of protein in the mycoplasma extracts (pmol$_e$/mg$_{prot}$). Mean ± SD from a minimum of two bio-replicates. T-test to compare results to WT sample (values considered statistically significant with two-sided P-value<0.05 are indicated with an asterisk; P-values are listed in Suppl. Table T1). Source and processed data provided in the Suppl. file F3.

The deletion of *mpn483* did not affect the GlcCer and GalCer levels but produced the most extreme phenotype with the loss of GGLs (no MGDAG, nor DGDAG) and a reduction of DHCer, while free DAG and ceramide increased two and a half and ten times, respectively (Fig. 3). These results suggest that the other glycosyltransferases (MPN028 and/or MPN075) could be responsible for synthesising MHCer, at least in the absence of MPN483, but they cannot use DAG as an acceptor substrate. In line with this, the deletion of *mpn028* did not render significant changes in any of the DAG forms, and only promoted a slight increase on the levels of free ceramide and DHCer and a two-fold increase in GlcCer. These results suggest that although *in vitro* studies pinpointed MPN075 as an inactive glycosyltransferase, in an *in vivo* context it might play a role in the synthesis of GlcCer, at least in the absence of MPN028. Alternatively, although *in vitro* results have shown that MPN483 prefers UDP-Galactose over UDP-Glucose as donor, and to extend the sugar chain rather than incorporating the first hexose into the glycolipids, MPN483 may synthesise GlcCer in the absence of MPN028.

The absence of galactolipids in strain Δ257 and the presence of GalCer in strain Δ483 was corroborated by dot blot using a commercial antibody against galactolipids (Suppl. Fig. S4).

The replacement of the *mpn483* gene by another glycosyltransferase with a preference for UDP-glucose restored the production of GGLs, yet the balance between MGDAG and DGDAG differed in each strain, being Δ483::GT the strain showing the phenotype more similar to WT (Fig. 3). All three strains, Δ483::GT, Δ483::AG and Δ483::SB, produce cerebrosides and DHCer, but again only Δ483::GT has a balance between these species similar to WT. All cerebrosides in these strains were GlcCer, except a tiny amount of GalCer in Δ483::AG, indicating that the three glycosyltransferases tested can use ceramide as a substrate and confirming their preference for UDP-glucose. Still, we cannot rule out the presence of galactolipids in any of these strains since we could not identify the carbohydrate moieties in most of the glycolipids.

The double deletion of *mpn257* and *mpn483* in strain Δ483Δ257 dramatically reduced most glycolipids favouring an excess of free ceramide and DAG, as in strain Δ483, and losing GalCer and increasing GlcCer like strain Δ257. This extreme phenotype is rescued by introducing MG517 in strain Δ483Δ257::prGT, which compensates for MPN483 activity and bypasses the absence of MPN257. This strain Δ483Δ257::prGT has WT levels of ceramide, and it only has GlcCer as its parental strain Δ257. Additionally, it restores WT levels of DGDAG, and other glycolipids show minimal differences to WT, the 20% reduction of DHCer being the most significant. Altogether, deleting *mpn257* prevents the production of galactolipids while replacing MPN483 with MG517 restores cell growth.

All strains have normal levels of the neutral lipids PC and TAG, with the only exception being the TAG increment in strain Δ483::GT (Suppl. Fig. S5). Ceramide, the precursor of cerebrosides, is the neutral lipid that showed more differences across strains. The excess of free ceramide is toxic for the cell (*i.e.*, it hardly mixes with other lipids, increases cell permeability, and destroys membrane asymmetry) [52,53], which could explain the reduction in the growth rate, especially in the most dramatic cases of strains Δ483 and Δ257Δ483.

3.5. Analysis of the cross-reactivity of the different strains with GalCer using acute phase serum from patients with GBS

Acute phase serum from patients with *M. pneumoniae* associated GBS (*Mp*GBS) is enriched in IgG anti-GalCer antibodies and cross-react with *M. pneumoniae* [9,22]. We first verified whether sera from *Mp*GBS and non-*Mp*GBS patients, healthy controls and intravenous immunoglobulin (IVIg) recognised *M. pneumoniae* derived glycolipids and observed strong IgG reactivity to *M. pneumoniae* glycolipid fractions in serum from *Mp*GBS (Suppl. Fig. 6). Next, we performed an inhibition ELISA assay to test whether cross-reactivity decreases with some of our engineered strains. To this end, anti-GalCer IgG positive sera from two *Mp*GBS patients were pre-incubated with different concentrations of whole-mycoplasma extracts and, subsequently, added to plates coated with commercial GalCer purified from bovine brains (Fig. 4A). The inhibitory potential of each extract was calculated using the same serum that was pre-incubated with buffer only (without mycoplasma extract) as reference (defined as 0% inhibition) (Fig. 4B). Sera from *Mp*GBS patients was also incubated with LOS from *C. jejuni* strains isolated from two patients (GB2 and GB19) [54] with *C. jejuni* associated GBS (*Cj*GBS) as a negative control of inhibition. Moreover, serum from a GBS patient with anti-GQ1b antibodies was pre-incubated with mycoplasma extracts and later exposed to ganglioside GQ1b to rule out non-specific depletion by mycoplasma extracts.

Most of the mycoplasma strains, but not the purified *C. jejuni* LOS, inhibited binding of *Mp*GBS sera to GalCer in a dose-dependent manner (Fig. 4B), demonstrating that depletion of GalCer recognising antibodies was specific to *M. pneumoniae* extracts. Of note, preincubation of *Mp*GBS sera with WT resulted in the strongest inhibition of GalCer recognition. Surprisingly, this inhibition was only partial in strain Δ257 whose lipidomic profile showed a complete absence of GalCer and should not have any

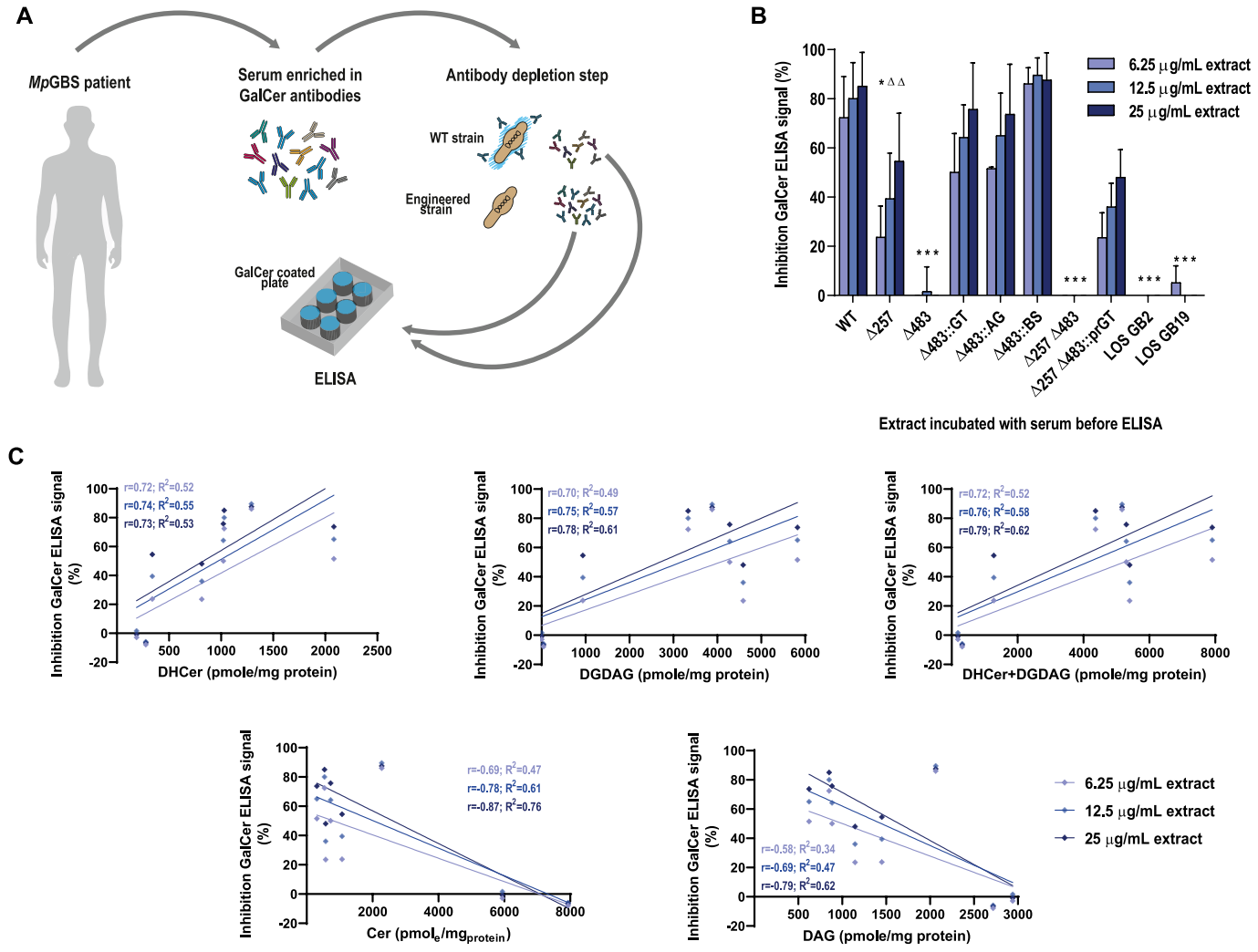

Fig. 4. Inhibition ELISA assay. (A) Scheme depicting the steps followed to evaluate cross-reactivity of IgG anti-GalCer positive *Mp*GBS sera with the engineered strains using an inhibition ELISA assay. Sera enriched in GalCer antibodies (blue shapes) is incubated with WT or engineered strains. The unbound fraction of these incubations is later added to GalCer coated plates to determine the recognition profile of *Mp*GBS sera to each strain **(B)** Cross-reactivity of IgG anti-GalCer with *M. pneumoniae* strains was assessed by incubating anti-GalCer reactive serum samples with increasing doses of whole-mycoplasma extracts of strains WT (M129), Δ257, Δ483, Δ483::GT, Δ483::AG, Δ483::SB, Δ257Δ483::prGT, Δ257Δ483 and two types of *C. jejuni* LOS (GB2 and GB19). Graph shows the mean ± SD percent inhibition compared to the reference (serum incubated with PBS without mycoplasma extract was defined as 0% inhibition) from a minimum of two biological replicas, obtained from two *Mp*GBS patient serum samples (see Suppl. Fig. S7. T-test to compare results to WT sample (values considered statistically significant with two-sided P-value<0.05 are indicated with an asterisk; and with P-value<0.001 with a triangle; P-values are listed in Suppl. Table T1). Source and processed data provided in the suppl. File F4. **(C)** Correlation of results from inhibition ELISA assays with the abundance of the indicated glycolipid species in the different strains. Pearson's correlation coefficient (r) and R-squared coefficient of determination (R^2) are shown for each linear regression calculated.

other galactolipid. Therefore, despite the lack of GalCer, there are still molecules on the surface of this strain that can deplete the pool of IgG anti-GalCer antibodies from *Mp*GBS sera. In contrast, strain Δ483 that shows normal levels of GalCer and GlcCer but barely any other glycolipid on its membrane completely lost the ability to inhibit the binding of *Mp*GBS sera to GalCer. A similar inhibition profile was observed for the double mutant strain Δ257Δ483. Regarding the KO strains complemented by other glycosyltransferases, strains Δ483::GT, Δ483::AG and Δ483::SB regained the ability to inhibit IgG binding to GalCer, in a manner comparable to the WT, whereas the complemented double mutant Δ257Δ483::prGT shows a partial inhibition profile similar to the Δ257 strain. Finally, none of the mycoplasma strains were able to significantly inhibit the recognition of GQ1b by GBS serum, ruling out non-specific depletion of antibodies by mycoplasma extracts (Suppl. Fig. S7). The inhibition assays were performed with sera from two *Mp*GBS patients and the mean of the results obtained with these two donors is plotted in Fig. 4. Similar patterns were observed when plotting the inhibition results from the two patients independently and the differences between strains were consistent between both donors (Suppl. Fig. S7).

Altogether the data suggest that the *M. pneumoniae* antigens responsible for the IgG cross-reactivity with GalCer may be other glycolipids than GalCer itself. As the engineered strains showed altered levels of several glycolipid species, we aimed to correlate the amount of each specific glycolipid with the inhibition results obtained with *Mp*GBS sera in the GalCer ELISA. We found that MHCer (both GlcCer and GalCer) and MGDAG levels do not correlate with the inhibition results (Suppl Fig. S8). In contrast, the inhibitory potential of the strains anticorrelates with Ceramide and DAG levels, and is positively correlated with DGDAG and DHCer levels (Fig. 4C). Specifically, the variants DGDAG and DHCer are strongly reduced in the Δ257 strain, which partially lost the ability to inhibit IgG binding to GalCer, and they are absent (except for a minor presence of DHCer) in the Δ483 strain, which is unable to deplete anti-GalCer signal from *Mp*GBS sera. Supporting the cross-reactivity of anti-GalCer antibodies with DHCer, *M. genitalium* and *M. agalactiae* extracts presented a similar inhibitory capacity as strain Δ257 while showing reduced levels of DHCer, but normal levels (if not increased) of DGDAG when compared to *M. pneumoniae* WT (Suppl. Fig. S9). Interestingly, these are two Mycoplasma species for which no association with GBS has been reported.

4. Discussion

Respiratory diseases are one of the most significant causes of death worldwide, and LBPs with lung specificity could lead to better therapies to improve prognosis. In this direction, we recently reported the first non-pathogenic bacterial chassis based on *M. pneumoniae*, which can dissolve biofilms made by *S. aureus* in catheters *in vivo* [4], locally deliver active enzymes to fight *Pseudomonas aeruginosa* infectious diseases in the lung [6] and decrease lung inflammation caused by infection [5]. Although the evidence of *M. pneumoniae* causing GBS is not as conclusive as for *C. jejuni*, it is desirable for a *M. pneumoniae* based chassis to bypass the GBS association.

The GalCer and other galactolipids with a terminal β-galactosyl residue in the *M. pneumoniae* surface are potential antigens that could trigger a cross-reactive antibody response to GalCer in human peripheral nerves causing GBS. Here, we engineered a set of *M. pneumoniae* mutant strains with the deletion or replacement of crucial enzymes for the biosynthesis of these galactolipids, according to the available literature and gene annotations [27,28,45,47,49–51].

Based on the glycolipid profiles of all the mutant strains analysed by LC-HRMS, we were able to refine the glycolipid metabolic map of *M. pneumoniae*. We confirmed that the *mpn257* gene encodes the only UDP-glucose epimerase in *M. pneumoniae*. We also corroborate the MPN483 activity observed *in vitro* [47] and show that the primordial function of MPN483 glycosyltransferase is to incorporate UDP-galactose or, to a lesser extent, UDP-glucose to GalCer in the production of DHCer, and it is the only enzyme synthesising GGLs (MGDAG and DGDAG). Moreover, our data suggest that the glycosyltransferase encoded by *mpn028* can synthesise MHCer (mainly GlcCer) but not DHCer nor GGLs. Thus, deletion of the *mpn257* gene abolishes the incorporation of galactose to ceramide or DAG, while deletion of the *mpn483* gene prevents the synthesis of any GGL and strongly reduces DHCer production. As expected, these two fitness gene deletions, especially the deletion of the *mpn483* gene, significantly impaired *M. pneumoniae* growth. The complementation of the *mpn483* gene deletion with similar glycosyltransferases with preference for UDP-glucose reverses the growth impairment, and strongly reduces (in the case of MGA_RS00300) or totally abolishes (in the case of MG517 or UgtP) the production of GalCer.

The evaluation of cross-reactivity of serum anti-GalCer IgG from *Mp*GBS patients with our mutant strains with modified glycolipid profiles revealed some unexpected results. The results for the engineered GalCer-negative *M. pneumoniae* strains (*i.e.*, those lacking *mpn257*), but also *M. genitalium* and *M. agalactiae* lacking GalCer, demonstrate that the anti-GalCer antibodies recognise other galactolipids from *Mycoplasma* aside from GalCer, possibly DHCer. Also, the partial cross-reactivity of the *Mp*GBS sera with strain Δ257 that lacks galactolipids suggests that the antibodies may also recognise glucolipids although with less affinity than galactolipids. In this direction, the complete lack of sera cross-reactivity with strain Δ483 with no DGDAG and barely detectable levels of DHCer supports the recognition of dihexoside glycolipids, probably with different carbohydrate moieties including galactose or glucose. However, we cannot discard that the lack of cross-reactivity of strain Δ483, which has WT levels of GalCer, derives from the abnormal levels of ceramide present in this strain. In this context, GalCer may not be properly oriented towards the outside of the membrane, explaining why this mutant is unable to deplete GalCer antibodies from *Mp*GBS sera.

Of note, in this study we used GBS sera from only two patients to investigate the cross-reactivity of anti-GalCer antibodies and *M. pneumoniae* strains. This is in part because GBS following an infection with *M. pneumoniae* is rare, especially in adults comprising the majority of our study cohort [22]. Nevertheless, similar results were obtained with the two sera that were used in this study, and the differences between strains were consistent. Importantly, we used sera collected before treatment with IVIg, which is the standard therapy for patients with GBS. IVIg contains antibodies to a wide variety of pathogens, and several mechanisms for the therapeutic action of IVIg have been proposed [55]. To rule out possible interfere of IVIg-derived *M. pneumoniae* reactive IgG in the inhibition assay we used pre-treatment sera. Finally, our results may also have broader implications as anti-GalC IgG antibodies are not restricted to patients with GBS and have also been detected in serum or cerebrospinal fluid from patients with encephalitis often with recent or concurrent *M. pneumoniae* infection [56,57]. It is possible that a similar cross-reactivity of IgG antibodies between GalC and *M. pneumoniae* antigens could play a role in *M. pneumoniae* associated encephalitis.

In summary, it seems several glycolipid species cross-react with sera from *Mp*GBS patients, particularly DHCer and DGDAG. However, it is unknown whether all these different glycolipids could act as triggering factors of GBS, or alternatively it is just GalCer the

triggering molecule and the antibodies generated show relaxed specificity for other glycolipid forms in our inhibition ELISA assay. Unfortunately, there are no animal models of GBS caused by *M. pneumoniae* to test the engineered strains described in this work, which might help elucidate the glycolipid form(s) triggering GBS linked to *M. pneumoniae* infection. In the case of *C. jejuni*-associated GBS, the antibodies are thought to be induced by the microbial antigen LOS, which shows an oligosaccharide core similar but not identical to oligosaccharides present in human ganglioside [54,58]. Hence, it might be possible that in *M. pneumoniae*-associated GBS, antibodies generated against DHCer and DGDAG (the main glycolipid species found to crossreact with *Mp*GBS patient sera), crossreact with GalCer and subsequently cause neurological disease. In this scenario, only strain Δ483 without any complementation, which shows a complete lack of DGDAG and barely detectable levels of DHCer, would bypass the association with GBS at the cost of a strongly reduced growth rate.

On the other hand, the fact that *M. genitalium* and *M. agalactiae* which show no, or very low levels of GalCer, can compete for the *Mp*GBS patient sera and in the case of *M. genitalium* there is no reported association to GBS, supports the hypothesis that recognition of DHCer and DGDAG by *Mp*GBS sera is the result of relaxed specificity of the antibodies in our inhibitory assay. This would suggest that GalCer is the only glycolipid form capable to trigger GBS. Indeed, it should be noted that antigen presentation of bacteria lacking lipopolysaccharide seems to occur via the CD1d receptor and the iNKT cells, which in turn activate B-cells to proliferate and produce immunoglobulins [59,60]. GalCer or GalDAG glycolipids but not GlcDAG bind and activate CD1d response [61–63]. It has been proposed that the immune response against *M. pneumoniae* might also be mediated by the CD1d receptor [47]. In this scenario, a strain with the deletion of the *mpn257* gene should prevent the induction of anti-GalCer antibodies associated with the autoimmunity of GBS since it is incapable of producing galactolipids. If *M. pneumoniae* could incorporate external galactose, the double deletion of *mpn257* and *mpn483* genes would ensure the galactolipid-free phenotype. However, in that case, it would be convenient to complement the glycosyltransferase activity, *e.g.* with the MG517 protein, to avoid growth impairment. These modifications enable the engineering of a non-pathogenic *M. pneumoniae* chassis, bypassing the association with GBS while maintaining a competitive growth rate. Furthermore, the resultant strains efficiently secrete therapeutic molecules, paving the way for the development of safer LBPs for the treatment of respiratory diseases.

Declaration of competing interest

The results published in this article are covered by patents PCT/EP2021/057122 and US2023/0310564 A1(licensed to Pulmobiotics S.L). L.S. and M.L.-S. are shareholders of Pulmobiotics S.L.. C.P.-L., R.M., and M.L.-S. are employees and have stock options of Pulmobiotics S.L. The remaining authors declare no competing interests.

Acknowledgments

This project has received funding from the European Research Council (ERC) under the European Union's Horizon 2020 research and innovation programme ERC LUNG-BIOREPAIR (101020135). We also acknowledge the support of the Spanish Ministry of Science and Innovation through the Plan Nacional PID2021-122341NB-I00 and the Centro de Excelencia Severo Ochoa (CEX2020-001049-S, MCIN/AEI /10.13039/501100011033), the Generalitat de Catalunya through the CERCA programme, the Center for Industrial Technology Development (CDTI) through the Neotec programme (SNEO 20211019) and to the EMBL partnership. C.P.-L. acknowledges the support of 'Programa Torres Quevedo' grant [PTQ2020-011048] funded by MCIN/AEI/10.13039/501100011033; European Union 'NextGenerationEU/PRTR'. The proteomics analyses were performed in the CRG/UPF Proteomics Unit which is part of the Spanish National Infrastructure for Omics Technologies (ICTS OmicsTech). We thank T. Hoogenboezem and C. Gago da Graça (Department of Pediatrics, Erasmus MC−Sophia Children's Hospital, University Medical Centre, Rotterdam, The Netherlands) for excellent technical assistance.

Appendix A. Supplementary data

Supplementary data to this article can be found online at https://doi.org/10.1016/j.micinf.2024.105342.

References

[1] Charbonneau MR, Isabella VM, Li N, Kurtz CB. Developing a new class of engineered live bacterial therapeutics to treat human diseases. Nat Commun 2020;11:1738.
[2] Sieow BFL, Wun KS, Yong WP, Hwang IY, Chang MW. Tweak to treat: Reprograming bacteria for cancer treatment. Trends Canc. 2021;7:447–64.
[3] Piñero-Lambea C, Ruano-Gallego D, Fernández LÁ. Engineered bacteria as therapeutic agents. Curr Opin Biotechnol 2015;35:94–102.
[4] Garrido V, Piñero-Lambea C, Rodriguez-Arce I, Paetzold B, Ferrar T, Weber M, et al. Engineering a genome-reduced bacterium to eliminate Staphylococcus aureus biofilms in vivo. Mol Syst Biol 2021;17:e10145.
[5] Montero-Blay A, Blanco JD, Rodriguez-Arce I, Lastrucci C, Piñero-Lambea C, Lluch-Senar M, et al. Bacterial expression of a designed single-chain <scp>IL</scp> -10 prevents severe lung inflammation. Mol Syst Biol 2023. https://doi.org/10.15252/msb.202211037.
[6] Mazzolini R, Rodríguez-Arce I, Fernández-Barat L, Piñero-Lambea C, Garrido V, Rebollada-Merino A, et al. Engineered live bacteria suppress Pseudomonas aeruginosa infection in mouse lung and dissolve endotracheal-tube biofilms. Nat Biotechnol 2023. https://doi.org/10.1038/s41587-022-01584-9.
[7] Narita M. Classification of extrapulmonary manifestations due to mycoplasma pneumoniae infection on the basis of possible pathogenesis. Front Microbiol 2016;7:23.
[8] Steele JC, Gladstone RM, Thanasophon S, Fleming PC. Mycoplasma penumoniae as a determinant of the guillain-barré syndrome. Lancet 1969;294:710–4.
[9] Ang CW, Tio-Gillen AP, Groen J, Herbrink P, Jacobs BC, Van Koningsveld R, et al. Cross-reactive anti-galactocerebroside antibodies and Mycoplasma pneumoniae infections in Guillain–Barré syndrome. J Neuroimmunol 2002;130:179–83.
[10] Willison HJ, Jacobs BC, Van Doorn P. Guillain-Barré syndrome. Lancet 2016;388:717–27.
[11] Sejvar JJ, Baughman AL, Wise M, Morgan OW. Population incidence of Guillain-Barré syndrome: a systematic review and meta-analysis. Neuroepidemiology 2011;36:123–33.
[12] Jacobs BC, Rothbarth PH, van der Meché FGA, Herbrink P, Schmitz PIM, de Klerk MA, et al. The spectrum of antecedent infections in Guillain-Barré syndrome. Neurology 1998;51:1110–5.
[13] Meyer Sauteur PM, Huizinga R, Tio-Gillen AP, Drenthen J, Unger WWJ, Jacobs E, et al. Intrathecal antibody responses to GalC in Guillain-Barré syndrome triggered by Mycoplasma pneumoniae. J Neuroimmunol 2018;314:13–6.
[14] Yuki N. Ganglioside mimicry and peripheral nerve disease. Muscle Nerve 2007;35:691–711.
[15] D'Angelo G, Capasso S, Sticco L, Russo D. Glycosphingolipids: synthesis and functions. FEBS J 2013;280:6338–53.
[16] Maggio B, Fanani ML, Rosetti CM, Wilke N. Biophysics of sphingolipids II. Glycosphingolipids: an assortment of multiple structural information transducers at the membrane surface. Biochim Biophys Acta 2006;1758:1922–44.
[17] Coet T, Suzuki K, , et alSuzuki K, Popko B, Suzuki K, Popko B. New perspectives on the function of myelin galactolipids. Trends Neurosci 1998;21:126–30.
[18] Yuki N, Susuki K, Koga M, Nishimoto Y, Odaka M, Hirata K, et al. Carbohydrate mimicry between human ganglioside GM1 and Campylobacter jejuni lipooligosaccharide causes Guillain-Barré syndrome. Proc Natl Acad Sci USA 2004;101:11404–9.
[19] Sharma MB, Chaudhry R, Tabassum I, Ahmed NH, Sahu JK, Dhawan B, et al. The presence of Mycoplasma pneumoniae infection and GM1 ganglioside antibodies in Guillain-Barré syndrome. J Inf Develop Countr 2011;5:459–64.
[20] Hao Q, Saida T, Kuroki S, Nishimura M, Nukina M, Obayashi H, et al. Antibodies to gangliosides and galactocerebroside in patients with Guillain-Barré syndrome with preceding Campylobacter jejuni and other identified infections. J Neuroimmunol 1998;81:116–26.

[21] Kusunoki S, Shiina M, Kanazawa I. Anti-Gal-C antibodies in GBS subsequent to mycoplasma infection: evidence of molecular mimicry. Neurology 2001;57:736–8.
[22] Meyer Sauteur PM, Huizinga R, Tio-Gillen AP, Roodbol J, Hoogenboezem T, Jacobs E, et al. Mycoplasma pneumoniae triggering the Guillain-Barré syndrome: a case-control study. Ann Neurol 2016;80:566–80.
[23] Meyer Sauteur PM, Huizinga R, Tio-Gillen AP, de Wit M-CY, Unger WWJ, Berger C, et al. Antibody responses to GalC in severe and complicated childhood Guillain-Barré syndrome. J Peripher Nerv Syst : JPNS 2018;23:67–9.
[24] Kuwahara M, Samukawa M, Ikeda T, Morikawa M, Ueno R, Hamada Y, et al. Characterization of the neurological diseases associated with Mycoplasma pneumoniae infection and anti-glycolipid antibodies. J Neurol 2017;264:467–75.
[25] Razin S. Structure and function in mycoplasma. Annu Rev Microbiol 1969;23:317–56.
[26] Plackett P, Marmion B, Shaw EJ, Lemcke RM. Immunochemical analysis of Mycoplasma pneumoniae: 3. Separation and chemical identification of serologically active lipids. Aust J Exp Biol Med Sci 1969;47:171–95.
[27] Himmelreich R, Hilbert H, Plagens H, Pirkl E, Li BC, Herrmann R. Complete sequence analysis of the genome of the bacterium Mycoplasma pneumoniae. Nucleic Acids Res 1996;24:4420–49.
[28] Yus E, Maier T, Michalodimitrakis K, van Noort V, Yamada T, Chen W-H, et al. Impact of genome reduction on bacterial metabolism and its regulation. Science 2009;326:1263–8.
[29] FDA. Early clinical trials with live biotherapeutic products: chemistry, manufacturing, and control information U.S. Department of Health and Human Services. Food and drug administration. Center for Biologics Evaluation an Research; 2016.
[30] Piñero-Lambea C, Garcia-Ramallo E, Miravet-Verde S, Burgos R, Scarpa M, Serrano L, et al. SURE editing: combining oligo-recombineering and programmable insertion/deletion of selection markers to efficiently edit the Mycoplasma pneumoniae genome. Nucleic Acids Res 2022. https://doi.org/10.1093/nar/gkac836.
[31] Montero-Blay A, Miravet-Verde S, Lluch-Senar M, Piñero-Lambea C, Serrano L. SynMyco transposon: engineering transposon vectors for efficient transformation of minimal genomes. DNA Res 2019;26:327–39.
[32] Pich OQ, Burgos R, Planell R, Querol E, Piñol J. Comparative analysis of antibiotic resistance gene markers in Mycoplasma genitalium: application to studies of the minimal gene complement. Microbiology 2006;152:519–27.
[33] Piñero Lambea C, Garcia-Ramallo E, Martinez S, Delgado J, Serrano L, Lluch-Senar M. Mycoplasma pneumoniae genome editing based on oligo recombineering and Cas9-mediated counterselection. ACS Synth Biol 2020. https://doi.org/10.1021/acssynbio.0c00022.
[34] Das S, Noe JC, Paik S, Kitten T. An improved arbitrary primed PCR method for rapid characterization of transposon insertion sites. J Microbiol Methods 2005;63:89–94.
[35] Gibson DG, Young L, Chuang R-Y, Venter JC, Hutchison CA, Smith HO. Enzymatic assembly of DNA molecules up to several hundred kilobases. Nat Methods 2009;6:343–5.
[36] Chiva C, Olivella R, Borràs E, Espadas G, Pastor O, Solé A, et al. QCloud: a cloud-based quality control system for mass spectrometry-based proteomics laboratories. PLoS One 2018;13:e0189209.
[37] Perkins DN, Pappin DJC, Creasy DM, Cottrell JS. Probability-based protein identification by searching sequence databases using mass spectrometry data. Electrophoresis 1999;20:3551–67.
[38] Beer LA, Liu P, Ky B, Barnhart KT, Speicher DW. Efficient quantitative comparisons of plasma proteomes using label-free analysis with MaxQuant. In: Methods in molecular biology, vol. 1619. Humana Press Inc.; 2017. p. 339–52.
[39] Perez-Riverol Y, Bai J, Bandla C, García-Seisdedos D, Hewapathirana S, Kamatchinathan S, et al. The PRIDE database resources in 2022: a hub for mass spectrometry-based proteomics evidences. Nucleic Acids Res 2022;50:D543.
[40] Simbari F, McCaskill J, Coakley G, Millar M, Maizels RM, Fabriás G, et al. Plasmalogen enrichment in exosomes secreted by a nematode parasite versus those derived from its mouse host: implications for exosome stability and biology. J Extracell Vesicles 2016;5.
[41] Barbacini P, Casas J, Torretta E, Capitanio D, Maccallini G, Hirschler V, et al. Regulation of serum sphingolipids in andean children born and living at high altitude (3775 m). Int J Mol Sci 2019;20:2835. *2019, Vol. 20, Page 2835*.
[42] Boutin M, Sun Y, Shacka JJ, Auray-Blais C. Tandem mass spectrometry multiplex analysis of glucosylceramide and galactosylceramide isoforms in brain tissues at different stages of Parkinson disease. Anal Chem 2016;88:1856–63.
[43] Meyer Sauteur PM, de Bruijn ACJM, Graça C, Tio-Gillen AP, Estevão SC, Hoogenboezem T, et al. Antibodies to protein but not glycolipid structures are important for host defense against mycoplasma pneumoniae. Infect Immun 2019;87:e00663. 18.
[44] Lluch-Senar M, Delgado J, Chen W-H, Lloréns-Rico V, O'Reilly FJ, Wodke JA, et al. Defining a minimal cell: essentiality of small ORFs and ncRNAs in a genome-reduced bacterium. Mol Syst Biol 2015;11:780.
[45] Miravet-Verde S, Burgos R, Delgado J, Lluch-Senar M, Serrano L. FASTQINS and ANUBIS: two bioinformatic tools to explore facts and artifacts in transposon sequencing and essentiality studies. Nucleic Acids Res 2020;48:e102.
[46] Razin S, Kutner S, Efrati H, Rottem S. Phospholipid and cholesterol uptake by mycoplasma cells and membranes. Biochim Biophys Acta Biomembr 1980;598:628–40.
[47] Rosén Klement ML, Öjemyr L, Tagscherer KE, Widmalm G, Wieslander Å. A processive lipid glycosyltransferase in the small human pathogen Mycoplasma pneumoniae: involvement in host immune response. Mol Microbiol 2007;65:1444–57.
[48] Razin S, Yogev D, Naot Y. Molecular biology and pathogenicity of mycoplasmas. Microbiol Mol Biol Rev : MMBR (Microbiol Mol Biol Rev) 1998;62:1094–156.
[49] Andrés E, Martínez N, Planas A. Expression and characterization of a mycoplasma genitalium glycosyltransferase in membrane glycolipid biosynthesis. J Biol Chem 2011;286:35367–79.
[50] Montero-Blay A, Piñero-Lambea C, Miravet-Verde S, Lluch-Senar M, Serrano L. Inferring active metabolic pathways from proteomics and essentiality data. Cell Rep 2020;31:107722.
[51] Jorasch P, Wolter FP, Zähringer U, Heinz E. A UDP glucosyltransferase from Bacillus subtilis successively transfers up to four glucose residues to 1,2-diacylglycerol: expression of ypfP in Escherichia coli and structural analysis of its reaction products. Mol Microbiol 1998;29:419–30.
[52] González-Ramírez EJ, Goñi FM, Alonso A. Mixing brain cerebrosides with brain ceramides, cholesterol and phospholipids. Sci Rep 2019;9:13326.
[53] Sarnyai F, Donkó MB, Mátyási J, Gór-Nagy Z, Marczi I, Simon-Szabó L, et al. Cellular toxicity of dietary trans fatty acids and its correlation with ceramide and diglyceride accumulation. Food Chem Toxicol 2019;124:324–35.
[54] Li T, Wolfert MA, Wei N, Huizinga R, Jacobs BC, Boons GJ. Chemoenzymatic synthesis of Campylobacter jejuni lipo-oligosaccharide core domains to examine Guillain-Barré syndrome serum antibody Specificities. J Am Chem Soc 2020;142:19611–21.
[55] Bayry J, Ahmed EA, Toscano-Rivero D, Vonniessen N, Genest G, Cohen CG, et al. Intravenous immunoglobulin: mechanism of action in autoimmune and inflammatory conditions. J Allergy Clin Immunol Pract 2023;11:1688–97.
[56] Christie L, Honarmand S, Yagi S, Ruiz S, Glaser C. Anti-galactocerebroside testing in Mycoplasma pneumoniae-associated encephalitis. J Neuroimmunol 2007;189:129–31.
[57] Meyer Sauteur PM, Jacobs BC, Spuesens EBM, Jacobs E, Nadal D, Vink C, et al. Antibody responses to mycoplasma pneumoniae: role in pathogenesis and diagnosis of encephalitis? PLoS Pathog 2014;10:e1003983.
[58] Laman JD, Huizinga R, Boons GJ, Jacobs BC. Guillain-Barré syndrome: expanding the concept of molecular mimicry. Trends Immunol 2022;43:296–308.
[59] Galli G, Nuti S, Tavarini S, Galli-Stampino L, De Lalla C, Casorati G, et al. Innate immune responses support adaptive immunity: NKT cells induce B cell activation. Vaccine 2003;21:S48–54.
[60] Kinjo Y, Tupin E, Wu D, Fujio M, Garcia-Navarro R, Benhnia MREI, et al. Natural killer T cells recognize diacylglycerol antigens from pathogenic bacteria. Nat Immunol 2006;7:978–86.
[61] Morita M, Motoki K, Akimoto K, Natori T, Sakai T, Sawa E, et al. Structure-activity relationship of alpha-galactosylceramides against B16-bearing mice. J Med Chem 1995;38:2176–87.
[62] Brigl M, van den Elzen P, Chen X, Meyers JH, Wu D, Wong C-H, et al. Conserved and heterogeneous lipid antigen specificities of CD1d-restricted NKT cell receptors. J Immunol 2006;176:3625–34.
[63] Parekh VV, Singh AK, Wilson MT, Olivares-Villagómez D, Bezbradica JS, Inazawa H, et al. Quantitative and qualitative differences in the in vivo response of NKT cells to distinct alpha- and beta-anomeric glycolipids. J Immunol 2004;173:3693–706.